$\mu = 6.1$ cm^{-1}. Space group $P2_1/c(C_{2h}^5)$ was uniquely established from the systematic absences: $0k0$ when $k \neq 2n$, $h0l$ when $l \neq 2n$.

Crystallographic Measurements. Preliminary unit cell parameters and space group information were obtained from oscillation and Weissenberg photographs taken with Cu Kα radiation. For intensity measurements, a crystal of dimensions ca. 0.16 × 0.26 × 0.50 mm was oriented on an Enraf-Nonius CAD-3 automated diffractometer (Ni-filtered Cu Kα radiation), where values for all unique reflections with $\theta < 67°$ were recorded by means of the θ–2θ scanning procedure as described previously.[22] A total of 1615 observed [$I > 2.0\sigma(I)$] intensities were corrected for the usual Lorentz and polarization effects and used in the structure analysis. Refined unit cell parameters were derived by least-squares treatment of the diffractometer setting angles for 40 reflections widely separated in reciprocal space.

Structure Analysis. The structure was solved routinely by direct methods using the MULTAN76[18] suite of programs. Approximate positions for all non-hydrogen atoms were obtained from an E map based on the largest 250 $|E|$ values and phases that yielded the highest combined figure of merit. Three cycles of full-matrix least-squares adjustment of atomic positional and isotropic thermal parameters reduced R[19] to 0.15 from a value of 0.26 for the initial model. Variation of hydrogen atom positional and isotropic thermal parameters in addition to non-hydrogen atom positional and anisotropic thermal parameters in the subsequent least-squares iterations converged to $R = 0.060$. Final non-hydrogen atom positional parameters are in Table III.[20] Anisotropic thermal parameters (Table V), hydrogen atom positional and thermal parameters (Table VI), and a list of observed and calculated structure amplitudes (Table VII) are available as supplementary material.[21]

Atomic scattering factors used in all structure factor calculations were those for carbon, nitrogen, and oxygen from ref 23 and for hydrogen from ref 24. In the least-squares iterations, $\sum w\Delta^2$ ($\Delta = ||F_o| - |F_c||$) was minimized, with weights, w, assigned according to the scheme: $w^{1/2} = 1$ when $|F_o| < 12.0$, and $w^{1/2} = 12.0/|F_o|$ when $|F_o| > 12.0$.

Acknowledgment. We thank the staffs of Analytical Research Services and the Department of Pharmacology for microanalyses, spectra, and biological testing. We are grateful to Professor Leon Mandell of Emory University for many helpful discussions.

Registry No. (±)-**2**, 82741-75-1; (±)-**3**, 82795-66-2; (±)-**3** (C_{52} epimer), 82795-67-3; (±)-**5a**, 82795-68-4; (±)-**5a** cyclic urethane, 82741-77-3; (±)-**5b**, 82741-76-2; (±)-**6a**, 82752-57-6; (±)-**6b**, 82796-02-9; (±)-**6c**, 82741-78-4; (±)-**6d**, 82741-79-5; **7**, 82741-80-8; (±)-**8a**, 82741-81-9; (±)-**8b**, 82795-69-5; (±)-**9**, 82741-82-0; (±)-**10**, 82741-83-1; (±)-**11**, 82741-84-2; (±)-**12**, 82741-85-3; (±)-**13**, 82741-86-4; (±)-**14**, 82741-87-5; (±)-**15**, 82741-88-6; (±)-**16**, 82741-89-7; (±)-**17**, 82741-90-0; (±)-**18**, 82741-91-1; 4-methoxybenzoyl chloride, 100-07-2.

Supplementary Material Available: Bond lengths and angles (Figure 2), tables of non-hydrogen atom fractional coordinates (Table III), torsion angles (Table IV), anisotropic thermal parameters (Table V) and hydrogen atom parameters (Table VI) (6 pages). Ordering information is given on any current masthead page.

Photochemical Three-Membered-Ring Cleavage of α-Cyclopropyl Ketones: A Theoretical Study

Alain Sevin* and Patrick Chaquin

Laboratoire de Chimie Organique Théorique, Université Pierre-et-Marie-Curie, Tour 44, 75230 Paris, Cedex 05, France

Received October 19, 1981

Ab initio SCF–CI calculations on cyclopropyl carboxaldehyde **3** have been carried out in order to simulate the various possibilities of ring cleavage induced by excitation of the CO chromophore. The preferential cleavage of the adjacent CC bond is interpreted in terms of the efficiency of the avoided crossing found along the potential energy surface of the lowest excited state. Selectivity as a function of conformation can be discussed by using simple perturbational arguments.

Owing to the pseudo π character of its Walsh MO's,[1] the cyclopropane ring interacts with an adjacent center bearing a p-type orbital. It has been shown, both experimentally[2] and theoretically,[3] that the strong conformational preference (about 18 kcal mol^{-1}) for a bisected conformation, **1a**, found in the cationic species results from a stabilizing two-electron two-orbital interaction. The stability difference between **1a** and **1b** is much less in the related cyclopropylcarbinyl radical,[4] but conformation **1a** is still prefered: three electrons are now involved in the dominant HOMO–LUMO interaction. On the same grounds, the related anion (four-electron interaction) is predicted to

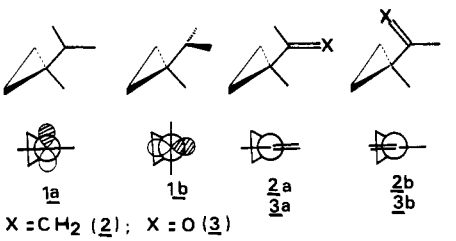

(1) The drawing of the classical Walsh MO's can be found in: W. L. Jorgensen and L. Salem, "The Organic Chemist's Book of Orbitals", Academic Press, New York, 1973.

(2) P. V. R. Schleyer and V. Buss, *J. Am. Chem. Soc.*, 91 5880–5882, (1969); V. Buss, R. Gleiter, and P. V. R. Schleyer, *ibid.*, **93**, 3927–3933 (1971). An extensive bibliography is given in these papers. See also B. Ree and J. C. Martin, *ibid.*, **91**, 5882–5883 (1969); **92**, 1660–1666 (1970).

(3) L. Radom, J. A. Pople, V. Buss, and P. V. R. Schleyer, *J. Am. Chem. Soc.*, **92**, 6380–6382 (1970), and references therein relative to other calculations. R. Hoffmann and R. B. Davidson, *ibid.*, **93**, 5699–5705 (1971). Conjugation into and through the cyclopropane ring has been studied (INDO) by L. D. Kispert, C. Engelman, C. Dyas, and C. O. Pittsman, Jr., *ibid.*, **93**, 6948–6953 (1971).

(4) W. J. Hehre, *J. Am. Chem. Soc.*, **95**, 2643–2646 (1973); H. J. Zimmerman, R. J. Buettcher, N. E. Buehler, G. E. Keck, and M. G. Steinmetz, *ibid.*, **98**, 7680–7689 (1976); I. M. Takakis and W. C. Agosta, *ibid.*, **101**, 2383–2389 (1979).

0022-3263/82/1947-4145$01.25/0

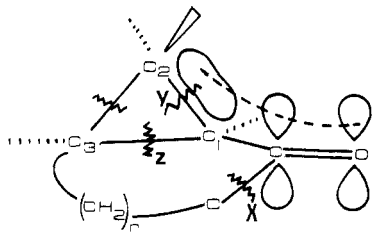

Figure 1. Model structure of the [4.1.0]heptanone. The numbers on the cyclopropane ring refer to the discussion.

adopt the conformation **1b**. The situation is more complex on considering vinylcyclopropane.[5] The π system of the double bond can be viewed as bearing one electron on the carbon bound to the ring and, at the same time, bearing an empty p orbital via the empty π^* MO. As an end result, the bisected conformation **2a** is slightly preferred (by about 3 kcal mol^{-1}). The same trends are expected from the cyclopropyl carboxaldehyde **3**. The actual polarization of the CO linkage C(δ+)–O(δ–) is likely to increase the weight of the cationic-type interaction. Preferential bissected conformations **3a** and **3b** have been deduced from NMR measurements.[6] The purpose of this study is to examine the changes brought about by this kind of conjugation on the photochemical behavior of α-cyclopropyl ketones.

The C_1C_2 photochemical cleavage of methylcyclopropyl ketone in the gas phase was first reported by Pitts and Norman:[7]

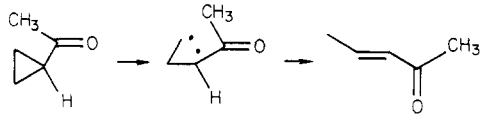

In a more recent paper, March and Pitts[8] present strong evidence that the reaction occurs through a vibrationally excited $^1n\pi^*$ state. A similar rupture was nevertheless observed via the triplet $^3n\pi^*$ state in the case of 2-spirocyclopropyl-1-indanone in rigid matrix.[9] Dauben et al. have illustrated the influence of conformation in a series of bicyclo[4.1.0]heptanones[10] (Figure 1). The observed selectivity of the C_1C_2 bond cleavage has been attributed to the overlap of the corresponding σ orbital with the π system of CO, in addition to least-motion considerations. A parallel study of bicyclo[3.1.0]hexanones has emphasized the role of substituents on overall selectivity.[11] On the grounds of experimental results, a selective weakening of the strained bonds has been proposed. In this perspective, the C_1C_2 vs. C_1C_3 selectivity would result from a complex balance between dynamic effects (assistance of the developing conjugation) and static effects (intrinsic bond strength). It is important to point out that the cleavage of the opposite C_2C_3 bond has never been observed though it has been reported in a few cases for the corresponding CO bond of the parent α-epoxy ketones.[12]

If one recalls that the ring–carbonyl bond is never cleaved under these conditions, the analogy with a conjugated system might be developed. But we must be aware of the fact that "conjugation" is a very general and vague term which is often at the source of conflicting interpretations. We will try in the following investigation to clearly depict this type of interaction in order to afford a simple standpoint allowing a general discussion. Unimolecular photochemical reactions will be treated in some detail.

Models and Methods

The aim of our study is mainly to provide an insight into the complex problem of weakly conjugated species. In this perspective, we will emphasize the role of perturbation interactions between the ring and the carbonyl using the familiar concepts of valence MO's and valence states. In other words, we mean that the various excited states, whose energies are obtained after configuration interaction (CI),[13] are depicted by their leading determinental configuration. Within this framework, the MO and state correlations can be assessed for limiting reactions, and the resultant topological description is relevant for predicting the existence (or not) and the nature of various kinds of potential energy barriers that one expects to find in the actual processes.[14] Indeed, this analysis is merely qualitative, but it has the merit of pointing out the important consequences of geometry variations on the electronic wave functions.

The simplest model of our study is cyclopropyl carboxaldehyde **3**. Keeping in mind the preceding remarks and looking at the great variety of reaction paths, we have adopted the following strategy: ab initio calculations have been carried out at two levels, (a) minimal STO-3G[15] basis (method I) and (b) minimal STO-3G augmented by diffuse functions on heavy atoms[16] (method II). Either the closed-shell Roothaan's Hamiltonian[17] or the "restricted" Nesbet's open-shell Hamiltonian[18] was used. The SCF step was followed by a CI involving the mono- and biexcited electronic configurations built on the six highest occupied and the five lowest unoccupied MO's. A set of 100 of the leading configurations was selected for the starting molecule and was then used to determine the CI energies of the various potential energy surfaces (PES's).

Despite of its simple formula, **3** possesses $3 \times 11 - 6 = 27$ internal degrees of freedom, so that the complete optimization of a given point along the reaction coordinate, even with method I, lies beyond the scope of this study. For practical reasons, and according to our initial strategy, we have adopted standard bond lengths for the starting molecule **3**;[19] then a linear variation of the geometrical parameters was assumed, between the initial molecule and the final target. The actual geometry changes will be

(5) W. J. Hehre, *J. Am. Chem. Soc.*, **94**, 6592–6597 (1972). See also A. De Meijeire and W. Luttke, *Tetrahedron*, **25**, 2047–2058 (1969).
(6) J. L. Pierre, *Ann. Chim. (Paris)*, 1, 383–388 (1966). Calculations (extended Hückel) have also been achieved by Hoffmann et al. in ref 3.
(7) J. N. Pitts, Jr., and I. Norman, *J. Am. Chem. Soc.*, **76**, 4815–4819 (1954). An exploratory work is found in H. E. Zimmerman and T. W. Flechtner, *ibid.*, **92**, 6931–6935 (1970), and references therein.
(8) D. G. Marsh and J. N. Pitts, Jr., *J. Am. Chem. Soc.*, **93**, 326–333 (1971); D. G. Marsh, J. N. Pitts, Jr., K. Schaffner, and A. Tuinman, *ibid.*, **93**, 333–338 (1971).
(9) R. O. Loufty and P. Yates, *J. Am. Chem. Soc.*, **101**, 4694–4698 (1979). See also D. R. Morton and N. J. Turro, *ibid.*, **95**, 3947–3957 (1973).
(10) W. G. Dauben, G. W. Shaffer, and E. J. Deviny, *J. Am. Chem. Soc.*, **92**, 6273–6281 (1970).
(11) W. G. Dauben, L. Schutte, G. W. Shaffer, and R. B. Gagosian, *J. Am. Chem. Soc.*, **95**, 468–471 (1973), and references therein.
(12) S. P. Pappas and L. Q. Bao, *J. Am. Chem. Soc.*, **95**, 7906–7907 (1973); J. Muzart, Thèse de doctorat d'état, No. AO 12684, University of Reims, France; A. Padwa, *Tetrahedron Lett.*, 816 (1964).
(13) By use of method I, for the starting molecule in its bisected conformation, the leading electronic configurations have coefficients of 0.93 and 0.92 in the normalized CI eigenfunction for the so-called $^3n\pi^*$ and $^1n\pi^*$ states, respectively; for more details, see Table I.
(14) A. Devaquet, A. Sevin, and B. Bigot, *J. Am. Chem. Soc.*, **100**, 2009–2011 (1978). A recent discussion is found in B. Bigot, A. Devaquet, and N. J. Turro, *ibid.*, **103**, 6–12 (1981).
(15) Using the GAUSSIAN 70 series of programs: W. J. Hehre, W. A. Lathan, R. Ditchfeld, M. D. Newton, and J. A. Pople, "Quantum Chemistry Program Exchange", Indiana University, Bloomington, IN, Program No. 236. The minimal STO-3G basis is described in W. J. Hehre, R. F. Stewart, and J. A. Pople, *J. Chem. Phys.*, **51**, 2657 (1969).
(16) Gaussian-type diffuse functions, with s and p exponents of 0.13, have been taken.
(17) C. C. J. Roothaan, *Rev. Mod. Phys.*, **23**, 68–89 (1951).
(18) R. K. Nesbet, *Rev. Mod. Phys.*, **35**, 552–557 (1963).
(19) Table of STO-3G standard bond lengths in J. A. Pople and M. Gordon, *J. Am. Chem. Soc.*, **89**, 4253–4261 (1967).

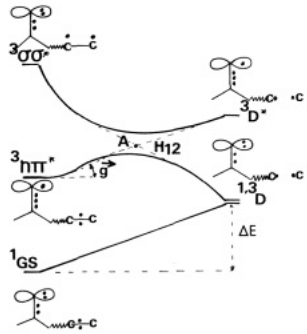

Figure 2. Schematic drawing showing the topicity of the rupture of a σ bond located at some distance from the CO chromophore. In the most general case, no symmetry element is present, and the crossing at point A is avoided. (The crossing is allowed when the bond is linked to the CO, as is the case for Norrish type I reaction.)

described in the discussion of the various reaction paths. Potential energy curves were obtained by calculating about 10 points for each process.

General Theoretical Considerations

Prior to a detailed analysis of cyclopropyl carboxaldehyde **3**, let us recall some useful generalities about topicity[20] of a σ bond cleavage induced by an n → π* excitation.

The scheme previously obtained for the classical Norrish type I reaction[21] is easily generalized to the case of any σ bond located at some distance of a carbonyl group. Let us denote $\sigma^2n^2\pi^2$ as the ground-state (GS) molecule (Figure 2). This state and the triplet state $\sigma^1n^2\pi^2(\sigma^*)^1$, of same topicity, are respectively linked to the singlet and triplet diradicals, while the low-lying triplet excited state $\sigma^2n^1\pi^2(\pi^*)^1$, of different topicity, is linked to an excited state of the final species. A surface crossing occurs at point A, which is more or less avoided in the absence of strong symmetry restrictions as in the case of the Norrish type I reaction itself. This simplified scheme allows us to point out the various energetic quantities that are of importance for the reactivity of the low-lying excited state. On the one hand we find *thermodynamic data* describing the positions of the starting and final states. On the other hand we have *electronic data* involving the gradient at the beginning of the reaction coordinate and a more complex quantity, H_{12}, reflecting the "ease" of the avoided crossing.[22]

Let us examine the competitive cleavages of a given molecule in a given state. Under the reasonable assumption that the various bonds of the same type are of comparable energy, the energy of the final moiety (and its relative position with respect to the starting system) is an important thermodynamic quantity since all paths have a common origin. The electronic factors are of different nature. The initial gradient is essentially related to a monodeterminental wave function (valence state) of the starting molecule. The H_{12} quantity is polydeterminental and results from the CI. Of course these quantities are not independent in a real process. But at a descriptive level one can say that the thermodymamics of the final species rather depicts the end of the reaction, the initial gradient characterizes its very beginning, and H_{12} controls the type of energy barrier. These arguments provide a guideline for the analysis of the conjugative effects, and we will use them in the following study.

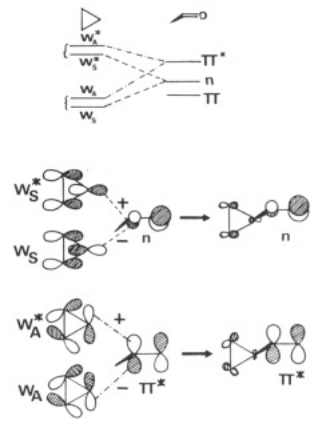

Figure 3. Interaction pattern for the building of n and π* MO's by starting from the cyclopropyl and the CO fragments. The interactions involving π MO's have not been added since the resulting MO is not used in the discussion.

Study of the Model Molecule 3

Molecular Orbitals. The main feature of the highest occupied and the lowest empty MO's are of special importance for the rest of the discussion. It is convenient to build them from two well-known interacting fragments: the cyclopropane ring and the carbonyl group. We will first restrict ourselves to the case of a C_s geometry, corresponding to the energy optimum, and we will then examine the changes brought about by conformational variations.

The MO scheme corresponding to the bisected conformation is drawn in Figure 3. The interactions yielding the HOMO–LUMO couple are outlined in the upper part, and the resulting MO's are shown in the lower part. With respect to the symmetry plane, two independent sets of MO's are considered. (a) The symmetrical one is concerned with the building of the HOMO, n, corresponding to the high-energy lone pair of the oxygen of the carbonyl. The symmetrical bonding and antibonding Walsh MO's of the cyclopropane ring (W_s and W_s*, respectively) are taken into account. (b) The antisymmetrical one is concerned with the building of the LUMO, π*, and involves the bonding and antibonding Walsh MO's (W_A and W_A*) of the ring.

In both cases, the fragment MO of the CO interacts in an out-of-phase fashion with W_A and in an in-phase fashion with W_A* (shown respectively by the minus and plus signs in Figure 3). (The relatives sizes of the lobes have been drawn somewhat schematically, for the purpose of emphasizing the phase relationships). As an end result, the leading features are as follows: the n MO (HOMO) bears bonding character between C_2 and C_3, while π* (LUMO) bears antibonding character between the same atoms. When the carbonyl group is moved from its C_s geometry by an angle θ, the preceding scheme has to be modified to account for the new mixings resulting from the loss of symmetry. Assuming that θ is small, the rotation does not significantly change the n MO since the C_1···CO bond and the n lone pair remain roughly parallel. But the situation is different in the previous antisymmetrical MO's. The corresponding changes are depicted in Figure 4. Repeating the phase rules of Figure 3, one gets the "rotated" π* MO which corresponds to (a) an increase of the antibonding character along C_1C_2 and (b) a dominant location on C_2 while the amplitude on C_3 is noticeably decreased.

(20) L. Salem, *J. Am. Chem. Soc.*, **96**, 3486–3501 (1974); W. G. Dauben, L. Salem, and N. J. Turro, *Acc. Chem. Res.*, **8**, 41–54 (1975).
(21) N. J. Turro, W. E. Farneth, and A. Devaquet, *J. Am. Chem. Soc.*, **98**, 7425–7427 (1976).
(22) L. Salem, C. Leforestier, G. Segal, and R. Wetmore, *J. Am. Chem. Soc.*, **97**, 479–487 (1975); A. Devaquet, *Top. Curr. Chem.*, **54**, 1–71 (1975); R. S. Mulliken, *J. Chem. Phys.*, **23**, 1833–1840, 1840–1846 (1955).

Table I. Comparison of the Calculated Values for Cyclopropanecarboxaldehyde and Reference Compounds[a]

molecule	state	leading confign(s)		rel energies method I	rel energies method II
3a	GS $^1A'$	$\cdots W_A^2\pi^2n^2$	0.98	0.0	0.0
	$^3n\pi^*$ $^3A''$	$\cdots W_A^2\pi^2n^1(\pi^*)^1$	0.93	100.9	123.6
	$^1n\pi^*$ $^1A''$	$\cdots W_A^2\pi^2n^1(\pi^*)^1$	0.92	118.1	137.2
	$^3\pi\pi^*$ $^3A'$	$\cdots W_A^2\pi^1n^2(\pi^*)^1$	0.73	123.4	151.6
		$\cdots W_A^1\pi^2n^2(\pi^*)^1$	0.59		
	$^1\pi\pi^*$ $^1A'$	$\cdots W_A^2\pi^1n^2(\pi^*)^1$	0.88	287.3	230.1
		$\cdots W_A^1\pi^2n^2(\pi^*)^1$	0.29		
H_2CO	GS $^1A_1$			0.0	0.0
	$^3n\pi^*$ $^3A_2$			72.0[b]	84.8[c]
				86.5[d]	86.5[d]
	$^1n\pi^*$ $^1A_2$			80.6[b]	98.6[d]
	$^3\pi\pi^*$ $^3A_1$			137.2[c]	133.2[d]
	$^1\pi\pi^*$ $^1A_1$				248.3[c]
CH_3CHO	GS $^1A'$			0.0	
	$^3n\pi^*$ $^3A''$			81.2	
	$^1n\pi^*$ $^1A''$			92.2[e]	
	$^3\pi\pi^*$ $^3A'$			127.5	
	$^1\pi\pi^*$ $^1A'$			242.2	

[a] The calculation has been carried out by using the same basis set and CI's of comparable sizes. The energies are in kilocalories per mole. The calculated reference energies are −226.92049 (method I) and −227.05345 au (method II) for 3a. [b] Reference 25. [c] Reference 23. [d] Reference 26. [e] Reference 27.

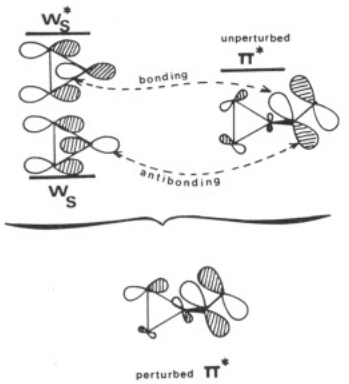

Figure 4. Scheme illustrating the mixing of the symmetrical and antisymmetrical Walsh MO's of the cyclopropyl ring when the carbonyl is slightly rotated. At the bottom of the figure one gets the resulting perturbed π^* MO, bearing an important p contribution on C_2, syn with respect to the carbonyl.

Both effects are summarized at the bottom of the figure.

Valence States. The various calculated energies of the low-lying vertical excited states of **3** in the bisected conformation are reported in Table I. The calculated values of $^{1,3}n\pi^*$ states and $^3\pi\pi^*$ states are comparable to those reported by Harding et al. for formaldehyde with an extended basis set.[23] The calculated energy of $^1\pi\pi^*$ is known to be overestimated by method I,[24] but we will see that, in reality, this state does not play any role in the description of reactivity. As expected, the introduction of diffuse orbitals (method II) stabilizes $^1\pi\pi^*$. An increase of the energy is also observed for $n\pi^*$ states. In this case, our calculation suffers from the limited size of the CI, since we introduce a larger set of virtual MO's. Let us now examine the energy changes as a function of θ for the GS and the lowest excited state $^3n\pi^*$.

(a) Ground State. As we have seen in Figure 3, the dominant stabilization occurs via the W_A–π_{CO}^* interaction (two electrons). This interaction decreases when θ increases and is zero for $\theta = 90°$; this is reflected in the total energy, and in going from $\theta = 0$ to $\theta = 90°$, a monotonous destabilization, reaching ~3 kcal mol^{-1} at 90°, is calculated. After 90° the energy decreases, but small changes are found (<1 kcal mol^{-1}). This value is not relevant in the absence of optimization.

(b) $^3n\pi^*$ Vertical Excited State. When one electron is transferred from n to π^*, the preceding interaction now involves three electrons, so that the stabilization is partly compensated but still decreases with increasing θ. As in the preceding case, a monotonous destabilization of the total energy is found, reaching ~2 kcal mol^{-1} for $\theta = 90°$.

Bond Strengths as a Function of θ in the Lowest Excited State. It is of interest to look at the consequences of the mixing schemes of Figures 3 and 4 with regard to the bond strengths of the CC bonds of the ring, since we have seen that the initial gradient along the reaction coordinate may eventually play a role in the description of the reactivity. It is reasonable to assume that at the very beginning of the cleavage, the reaction coordinate "looks like" a simple valence stretching. When $\theta = 0$, the lowest triplet wave function is mainly monodeterminental, the coefficient of the HOMO → LUMO excitation being 0.93 in the CI eigenfunction (see Table I). This situation persists when θ is changed up to 180°. Thus the electronic density variation occurring in this couple of MO's provides a picture of the overall electronic density variation. Though Mulliken's populations,[28] after CI, have been taken as indices of the CC bond strengths and interpreted in terms of perturbation theory restricted to the HOMO–LUMO couple, one has to note that the related absolute values have no physical signification, but the relative variations are indicative of the main electronic changes.

Coming back to **3** in its bisected conformation **3a**, we see that the promotion of one electron from n removes bonding density between C_1 and C_2, while the partial filling of π^* pours antibonding density between the same atoms. If the bonds are frozen, a neat destabilization of C_2C_3 results, with respect to C_1C_2 and C_1C_3. This is corroborated by the calculated overlap populations shown in Figure 5 and leads to a paradoxical finding: the C_2C_3 bond, which

(23) L. B. Harding and W. A. Goddard III, *J. Am. Chem. Soc.*, **99**, 677–683 (1977).
(24) C. F. Bender, T. H. Dunning, Jr., H. F. Schaefer III, W. A. Goddard III, and W. J. Hunt, *Chem. Phys. Lett.*, **15**, 171–178 (1972).
(25) J. D. Goddard and H. F. Schaefer III, *J. Chem. Phys.*, **70**, 5117–5134 (1979).
(26) A. Sevin, B. Bigot, and A. Devaquet, *Tetrahedron*, **34**, 3275–3280 (1978).
(27) The authors, unpublished results.
(28) S. Winstein and E. M. Kosower, *J. Am. Chem. Soc.*, **78**, 4354–4408 (1959).

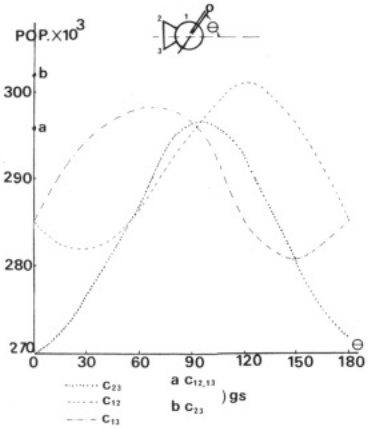

Figure 5. Mulliken's electronic populations of the lowest excited state[3] $n\pi^*$, calculated after CI, as a function of θ. The points a and b are the populations of C_1C_2 (C_1C_3) and C_2C_3, respectively, in the ground state of the molecule.

is never cleaved photochemically, possesses the lowest electron density in the vertical excited state. This is not the case in the GS where the transfer $W_A \rightarrow \pi_{CO}^*$ weakens C_1C_2 and C_1C_3 but strengthens C_2C_3, as in the related cyclopropylcarbinyl cation. Indeed, the electronic populations are respectively 0.296 and 0.302 for C_1C_2 and C_2C_3 (points a and b on Figure 5).

The conformational changes introduce important variations in the relative bond strengths.

(a) C_2C_3 Bond. We have seen previously that the mixing of π_{CO}^* with W_A and W_A^* introduces antibonding character between C_2 and C_3 (Figure 3). This interaction is strong when $\theta = 0$ or 180° and vanishes when $\theta = 90°$. It follows that, when π^* is populated, the bond strength is minimum for $\theta = 0°$ or 180° (maximum antibonding character between C_2 and C_3) and is maximum for $\theta = 90°$ (no antibonding character between C_2 and C_3).

(b) C_1C_2 (Syn) Bond. We have noticed in Figure 4 that a small twisting introduces a perturbation which increases the antibonding character along C_1C_2, and, as a matter of fact, an initial destabilization of this bond is observed, increasing up to $\theta = 30°$. For $30° < \theta < 90°$, the mixings of the symmetrical set (W_S, W_S^*) and the antisymmetrical set (W_A, W_A^*) compete. The W_S/W_S^* interaction becomes important and the loss of the W_A/W_A^* interaction decreases the antibonding character. For $\theta > 90°$, the situation is analogous to that previously found in the 90–0° interval by permuting the roles of C_1C_2 and C_1C_3, and the electronic population of C_1C_2 reaches a maximum for $\theta = 120°$.

(c) C_1C_3 (Anti) Bond. The situation is similar to that of C_1C_2, but instead of θ we have to consider $180 - \theta$. A minimum is found for 150°, and the electronic population then increases up to 60° and finally decreases when θ reaches 0°.

It is noteworthy that for $\theta = 90°$, the three electronic populations are equal; that is to say, the overall conjugation effects are nul or compensate each other for the various ring bonds.

Let us briefly summarize the various trends depicting the electronic changes in the three-membered-ring bonds in the lowest excited state: (a) A paradox is found, the C_2C_3 bond is the most affected by the excitation process and is the weakest in the bisected conformations ($\theta = 0°$ and 180°). (b) An important conformational dependence is found. It is of the same order of magnitude as the electronic density changes brought about by the excitation (see the relative variations in Figure 5). (c) For small torsional angles (around 30°) C_2C_3 and C_1C_2 have comparable strengths and are weaker than C_1C_3. The difference between C_1C_2 and C_1C_3 results from both mixings with the symmetrical Walsh MO's (W_s and W_s^*), which increases as sin θ increases, and with the antisymmetrical Walsh MO's (W_A and W_A^*), slowly decreasing as cos θ decreases. It follows that the difference is rapidly increasing for small values of θ. (d) The behavior of C_1C_2 and C_1C_3 is quite symmetrical when one changes θ into $180 - \theta$, respectively.

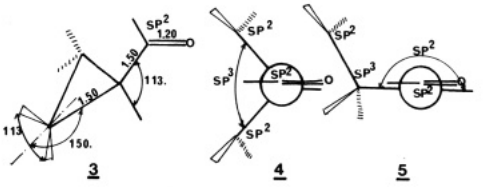

Figure 6. Model structures used in the calculations.

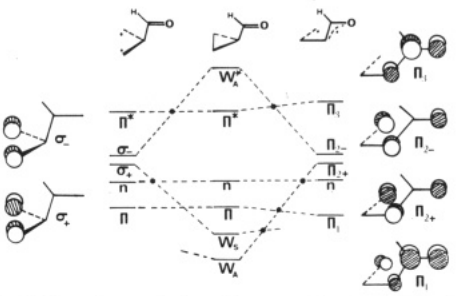

Figure 7. Natural correlation diagram for the MO's during the rupture of C_2C_3 (left side), where the C_s symmetry is preserved, and the rupture of C_1C_2 (right side), where no symmetry element is present. The actual correlations, at the SCF level, are obtained when the avoided crossings represented by dots are taken into account. The resulting correlations have not been drawn for the sake of clarity.

These findings cannot explain the experimental photochemical reactivity which is observed. For small values of θ, ranging from 0° to 30°, as is the case in the bicyclo[4.1.0] and bicyclo[3.1.0] series, the C_2C_3 cleavage is never observed, and C_1C_2 is broken very preferentially (see the introduction). It follows that the eventual "initial gradient" argument has to be seriously questioned and is not very likely to be a determinant in dealing with the overall reactivity. This point will be discussed in more detail later on.

Comparative Model Studies of C_1C_2/C_2C_3 Ruptures

The two limiting reactions of **3**, yielding **4** and **5**, respectively (Figure 6), will be first examined by using the natural MO correlation method,[14] in order to emphasize the number and the nature of the crossings along the various PES's.

C_2C_3 Rupture. This reaction have been simulated by progressive opening of the $C_2C_1C_3$ angle, preserving the symmetry plane of the bisected conformation **3a**, and yielding the intermediate **4**.

(a) MO Correlations (Left Side of Figure 7). The correlations of the Walsh MO's have already been discussed in detail[29] and do not deserve special comment: the bonding W_s and antibonding W_A^* MO's tend to yield σ_+ and σ_-, in-phase and out-of-phase combinations of p lobes on C_2 and C_3, respectively. In terms of natural MO correlations[14] the identity of n,π,π^* is preserved. When the

(29) R. Hoffmann, *J. Am. Chem. Soc.*, **90**, 1475–1485 (1968); J. A. Horsley, Y. Jean, C. Moser, L. Salem, R. M. Stevens, and J. S. Wright, *ibid.*, **94**, 279–282 (1972).

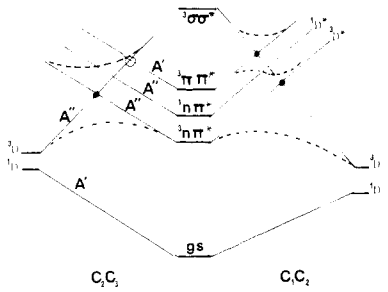

Figure 8. State correlation diagram resulting from the natural MO correlations of Figure 7. Once the avoided crossings are taken into account, one obtains the behavior depicted by the broken lines. For example, $^3n\pi^*$ is linked to ^3D via a nonmonotonous correlation.

symmetry restrictions are taken into account, two avoided MO crossings result (dots). The final n–σ_+ correlation thus involves an important change of electronic localization: from the oxygen atom to the C_2,C_3 carbons.

(b) State Correlations (Left Side of Figure 8). The description of the low-lying states of **4** is greatly facilitated by the concept of the "homosymmetric diradical" introduced by Salem et al.[30] Referring to Figure 7, we can consider to a first approximation that the σ_+/σ_- couple is typical of such a species. In fact, these MO's are not only localized on the methylenes, and, more especially, σ_- bears a nonnegligible contribution of the other heavy atoms. The "ideal" $1/2^{1/2}$ (HOMO^2–LUMO^2) covalent diradical eigenfunction is noticeably "distorted", and indeed the lowest singlet state has the dominant contributions: $0.81\sigma_+^2 - 0.54\sigma_-^2$ + minor terms. The corresponding triplet has the pure configuration $^3(\sigma_+{}^1\sigma_-{}^1)$ (=0.99). We call these states $^{1,3}D$ in order to outline their dominant diradical character: each unpaired electron is located on a methylene. The singlet configuration $^1(\sigma_+{}^1\sigma_-{}^1)$, which corresponds to the Z_1 zwitterion of Salem's notation is found 8 eV above $^{1,3}D$ and will not be taken into account. The $^3\pi\pi^*$ excited state of the final species is also found at very high energy (excited diradical).

The correlations of the low-lying states are now easy to obtain: the GS is linked to ^1D and $^3n\pi^*$ to ^3D. The correlation of the triplet state is not monotonous (broken lines) since we have seen that avoided crossings occur along the HOMO and LUMO correlations. (The intended correlations are indicated by heavy lines.) In a similar fashion, $^1n\pi^*$ is linked to a high-energy species. Due to the symmetry constraints, the correlation of $^3\pi\pi^*$ does not interfere with the $^3n\pi^*$ one.

C_1C_2 Rupture. In this type of cleavage, no symmetry element is preserved along the reaction coordinate: the $C_1C_3C_2$ angle is opened up to a final sp^3 geometry. In the open species **5**, the C_3C_1HCHO atoms have been taken to be coplanar, allowing allylic conjugation.

(a) MO Correlations (Right Side of Figure 6). With respect to the former analysis, two new facts emerge: the bonding Walsh MO which is destabilized is W_A; due to the formation of an allylic species, the former $\pi\sigma_+\sigma_-\pi^*$ set is replaced by the sequence $\pi_1\pi_{2+}\pi_{2-}\pi_3$. The HOMO–LUMO couple π_{2+} and π_{2-} is built by mixing in phase and out of phase, respectively, the π_2 allyl-type MO and a p orbital on C_2.

The natural correlations are self-evident (dotted lines), and once taking into account the avoided crossings, we note the following. (1) The n MO is now correlated with π_{2+}, and the corresponding electronic changes are much less drastic than in the previous reaction, both MO's bearing an important contribution on the oxygen atom. In terms of electron density, the avoided crossing corresponds to a 90° rotation of the oxygen p lobe (from the n to the π local plane). (2) Within the occupied MO's, a corresponding $\pi \rightarrow$ n rotation is observed. (3) An avoided crossing is found in the empty MO's.

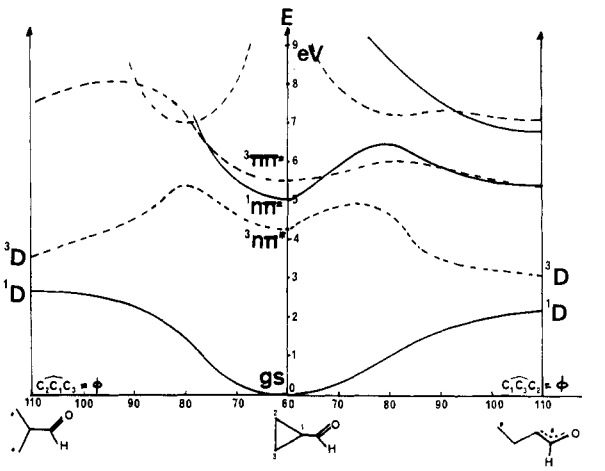

Figure 9. Calculated PES's for the model reaction paths. The reaction coordinate is complex and ϕ only symbolizes the progress of the overall process.

(b) State Correlations. The preceding type of discussion remains valid for this type of reaction, but the nature of the low-lying valence states of the final species has to be precised.

According to the MO scheme of Figure 6 (right part), the frontier orbitals of the open species, namely π_{2+} and π_{2-}, can be used, here again to a first approximation, to describe a kind of diradical moiety. The lowest singlet eigenfunction is $0.8\ \pi_{2+}^2 - 0.52\ \pi_{2-}^2$ + terms < 0.09. The lowest triplet has the pure configuration $^3(\pi_{2+}{}^1\pi_{2-}{}^1)$ (>0.97) and is found at the same energy. These configurations correspond to the coupling of an allyl radical and a methylene radical in a singlet and triplet fashion, respectively.

As in the C_2C_3 rupture, the GS is linked to the singlet diradical ^1D; $^3n\pi^*$ is linked to ^3D via a nonmonotonous correlation, and $^1n\pi^*$ is linked to a high-energy singlet state of the final species. The behavior of $^3\pi\pi^*$ is complex. As a result of an avoided crossing with an upper dissociative state symbolized by $^3\sigma\sigma^*$, the correlation of $^3\pi\pi^*$ exhibits a sinuous shape. This state keeps formally the "memory" of two avoided crossings as indicated by broken lines.

Discussion of Reactivity

Calculated Curves. Calculated curves are shown in Figure 9. For the C_2C_3 rupture, the initial molecule was taken to be in its **3a** conformation, yielding the open form **4** (Figure 6). For the C_1C_2 rupture, the curves reported on Figure 10 correspond to the most favorable conformation, $\theta = 30°$, the final species **5** (Figure 6) allowing allylic conjugation along C_1CO. In both cases, a linear variation of angles and dihedra has been assumed whereas bond lengths have been kept at their initial value. These model limiting processes obviously suffer from severe constraints. The calculated activation energies obtained this way are not very accurate; however, two remarks can be made. (1) Using these crude methods, we find that the lowest excited-state PES maxima occur for relatively small vlaues of the opening angle (Φ), around 10–15°; thus, the eventual bond relaxation is not expected to be important before the "tophill" of the reaction coordinate. (2) With these as-

(30) L. Salem and C. Rowland, *Angew. Chem., Int. Ed. Engl.*, 11, 92–111 (1972).

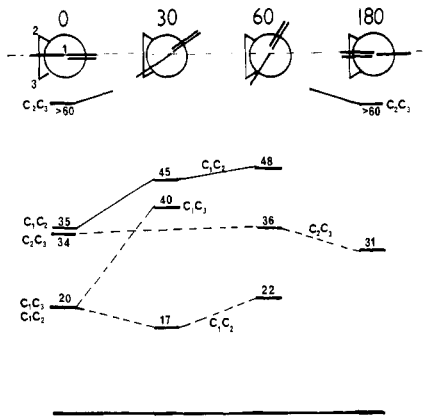

Figure 10. Calculated activation energies for several values of θ: broken lines, $^3n\pi^*$; full lines, $^1n\pi^*$ (kcal/mol).

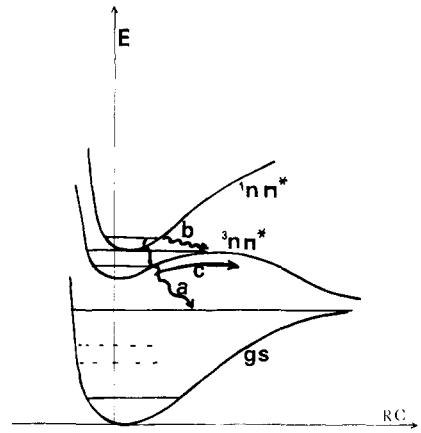

Figure 11. Scheme illustrating the various reaction possibilities of the lowest excited states of the system. The horizontal lines are only drawn to recall that vibrationally excited states of the molecule are involved in the real process, especially dealing with the GS.

sumptions the actual activation energies are supposed to be smaller than our calculated values that remain, however, comparative landmarks.

These energies have been reported in Figure 10 for several initial conformations of **3** and for several types of cleavages and will be used in the following discussion.

C_1C_2 vs. C_2C_3 Cleavage Selectivity. The problem of the preferential C_1C_2 or C_2C_3 bond rupture will be examined by using the three criteria we have previously selected: thermodynamic data of the final species, initial increasing of the reactive state potential energy along the reaction coordinate, and the nature and number of avoided crossings.

The initial gradient does not seem to be the leading criterion, since we have seen that in the frozen molecule, the C_2C_3 bond has the lowest electronic population in the $n\pi^*$ excited state. The conjugation of the final species **5**, which stabilizes it by 8 kcal mol^{-1} with respect to **4**, does not play an important role because it is noticeable only at the end of the reaction, rather far from the transition region. Though the topology of the PES's appears to be prominent, we have seen that, during the C_2C_3 rupture, the avoided MO crossing along the HOMO–LUMO correlation corresponds to an important location change in the wave-function amplitude, while it is smoother for the C_1C_2 rupture due to a better overlap. Hence, the related H_{12} term is larger for this rupture, and, moreover, the loss of symmetry induces a second avoided crossing between the dissociative $^3\sigma\sigma^*$ type and the $^3\pi\pi^*$ states. The resulting situation is more diffuse, and the energy barrier is lowered for the lowest PES.

C_1C_2 vs. C_1C_3 Selectivity as a Function of the Conformation. In these two types of cleavage, the thermodynamic conditions are the same, and the topology of the PES's is very similar. Then, the main source of selectivity appears to be the initial gradient along the $n\pi^*$ state. Indeed, there is a parallelism between the calculated activation energies for C_1C_2/C_1C_3 ruptures and their respective electronic population (Figure 6). The $\theta = 30°$ conformer is the most favorable for C_1C_2 cleavage; this conformer also corresponds to a least-motion path, since the value of θ does not change along the reaction path.

Singlet Reactivity. Due to the energy barrier that this state has to overcome before reaching the final species, the $^1n\pi^*$ state is not expected to be directly reactive. Two hypothetical reactive channels nevertheless remain likely.

The first one consists of a nonradiative deactivation yielding a hot ground state whose excess of vibrationnal energy would be able to drive the reaction along the GS PES, as schematically indicated in Figure 11 by arrow a. This process is a priori feasible in the gas phase if one looks at the relative energies of $^1n\pi^*$ and ^1D; in condensed media, the exchange of energy with the partners would render this process very unlikely.

The second one involves an intersystem crossing from $^1n\pi^*$ to $^3n\pi^*$, around the maximum of the triplet PES. This surface "switching" is facilitated by the presence of the upper $^3\pi\pi^*$ state according to Lee's formulation of the transition matrix for intersystem crossing, based on the early work of Lin.[31] For the three states S_1, T_2, and T_3 the probability of the $T_2 \rightarrow S_1$ transition is increased by a perturbing T_3 state lying close to S_1. (The corresponding coupling is complex: S_1 and T_3 are coupled via the spin–orbit operator while T_2 and T_3 are coupled via a vibronic term; at the present time, we cannot evaluate its magnitude.)

Triplet-State Reactivity. The energy barrier corresponding to C_1C_2 cleavage along the $^3n\pi^*$ PES is small, even at our level of calculations; it is then anticipated that the corresponding reaction is feasible within the lifetime of the triplet state (arrow c of Figure 11). The resulting species lies in a potential well which renders the reverse reaction very unlikely via this state; the two evolution channels consist of either a subsequent reaction of the open species or an intersystem crossing leading to the singlet GS species followed by an exothermal ring reclosure. It can be anticipated that irradiation of this molecule in the presence of heavy-atom solvents will favor the reaction in the triplet state, leading to dominant C_1C_2 cleavage.

The exploratory scans of the various PES's that have been done allow qualitative considerations on the important electronic factors that rule the overall reactivity: (1) Upon HOMO/LUMO vertical excitation, the C_2C_3 bond strength is noticeably weakened, with respect to the other ring bonds, in the bisected conformation. This situation no longer persists when the carbonyl group is rotated and the three-bond populations are equal at $\theta = 90°$. (2) Although the various conjugative effects arising between the cyclopropane and the CO chromophore are weak, they play a prominent role during the cleavage: the electronic factors intervening in the avoided crossing of the lowest excited PES make the C_1C_2 cleavage smoother than the C_2C_3 one. Roughly speaking, the overlap of the crossing surfaces, i.e., of the states built on the MO's representing the σ bond and the carbonyl, is better for C_1C_2 than for C_2C_3. (3) The C_1C_2/C_1C_3 bond rupture selectivity, in the excited state,

(31) A. Devaquet, A. Sevin, and B. Bigot, *J. Am. Chem. Soc.*, **100**, 2009–2011 (1978).

is mainly controlled by a conformational dependence, already found in the starting molecule. It can be anticipated that upon an increase of the temperature the selectivity will decrease due to the leveling of the various conformer populations. At any rate, the cleavage of these bonds will remain preferential due to the greater stability of the final system.

We have seen in Figures 9 and 10 that in all cases energy barriers are found along the low-energy excited-state PES's. We thus conceive that the ring cleavage might compete with other reactive processes of the excited carbonyl, more especially with Norrish type II reactions for open-chain aliphatic compounds and Norrish type I for alicyclic compounds.[10] It is noteworthy that calculated energies of these reactions obtained by a similar method[26,31,32] lie in the same energetic range.

The case of [3.1.0] and [4.1.0] derivatives deserves some comment, and we will use the nomenclature of Dauben et al.[11] shown in Figure 1 in the following discussion.

(a) [3.1.0] Derivatives. In Figure 10 we have seen that for $\theta = 30°$, in our strain-free model, the Y rupture is preferred to the Z rupture by 13 kcal mol^{-1}. The presence of a noticeable ring strain might be of the same order of magnitude and might decrease the activation energy of the Z rupture. The reaction products will result from a competition between X, Y, and Z ruptures, and the relative stability of the various open intermediates is likely to rule the final product distribution.

(b) [4.1.0] Derivatives. The situation is clearer than for the preceding series for now the system might be considered as strain free. As can be seen in Figure 10, the Y (C_1C_2) rupture is the easiest for realistic values of θ and the product distribution will be ruled by the competition between the Y and the Norrish type I cleavages.

Acknowledgment. This study was initially suggested by Professor J. P. Pete, Reims University. We are greatly indebted to Professor J. P. Pete and Dr. J. Muzard for many stimulating discussions we had during the course of this work.

(32) H. Cardy, E. Poquet, M. Chaillet, and A. Dargelos, *Nouv. J. Chim.*, 2, 603-608 (1978).

Preparation and Diels-Alder Reactions of 1,1-Dicarbonylalkenes

Thomas R. Hoye,* Andrew J. Caruso, and Andrew S. Magee

Department of Chemistry, University of Minnesota, Minneapolis, Minnesota 55455

Received October 6, 1981

1,1-Dicarbonyl- (ester, ketone, lactone) substituted alkenes are prepared from the corresponding saturated 1-phenylsulfinyl derivatives. These are formed from precursor sulfides, which can be efficiently prepared either by oxidation of β-hydroxy-α-phenylsulfenylcarbonyl compounds or direct acylation of α-phenylsulfenyl enolate anions with acid chlorides. Some of the title compounds can be isolated and then reacted while others are generated and reacted in situ in a Diels-Alder fashion with cyclopentadiene. Endo-exo selectivities are discussed.

In a current study in our laboratory the intramolecular Diels-Alder chemistry of dienophilic 1-carbomethoxy-1-ketoalkenes is being investigated. In connection with this work, methods for the preparation of these dienophiles and their precursor sulfoxides[1] have been developed, and some intermolecular Diels-Alder reactions[2] of the title compounds have been examined. Those observations are described here.

A synthesis of the 1,1-dicarbonyl-substituted alkenes (**1**) by thermolysis of a 1-sulfinyl precursors **2** seemed advantageous since it would allow generation of **1**, a molecule potentially prone to polymerization, in the presence of Diels-Alder dienes. It would also allow for the construction of these precursors via carbon-carbon bond-forming reactions. For example, we recently reported[3] a zinc chloride assisted aldol reaction of α-phenylthio ester enolate anions with aldehydes to generate β-hydroxy-α-phenylthio esters (**3**). Successful oxidation of the alcohols **3** to ketones **4** would enable the application of this chemistry to our needs

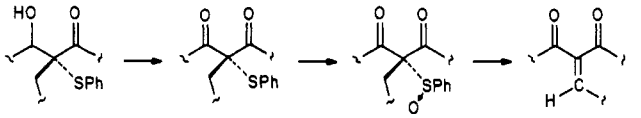

3 **4** **2** **1**

since **4** could, of course, yield **2** and **1** upon oxidation and elimination of the sulfur. This scheme was reduced to practice as outlined in Table I. The β-hydroxy lactones **3a-d** and ester **3e** were prepared by the previous method.[3] Oxidation to the keto sulfides **4a-c** and **4e** could be effected either with dimethyl sulfoxide/trifluoroacetic anhydride[4] or Me_2SO/oxalyl chloride[5] without interference by sulfur oxidation.[6] An alternative method for prepa-

(1) The preparation and Michael reactions of di-*tert*-butyl methylenemalonate and *tert*-butyl 2-acetylacrylate were recently described: Baar, M. R.; Roberts, B. W. "Abstracts of Papers", 181st National Meeting of the American Chemical Society, Atlanta, GA, March 1981; American Chemical Society: Washington, D.C., 1981; ORGN 83.

(2) Both the Diels-Alder reactivity and facile preparation of some cyclic, unsaturated β-dicarbonyl compounds have been recently described: Liotta, D.; Saindane, M.; Barnum, C. *J. Am. Chem. Soc.* **1981**, *103* 3224. Liotta, D.; Barnum, C.; Puleo, R.; Zima, G.; Bayer, C.; Kezer, H. S., III *J. Org. Chem.* **1981**, *46*, 2920. Liotta, D.; Saindane, M.; Barnum, C.; Ensley, H.; Balakrishnan, P. *Tetrahedron Lett.* **1981**, 3043.

(3) Hoye, T. R.; Kurth, M. J. *J. Org. Chem.* **1980**, *45*, 3549.

(4) Huang, S. L.; Omura, K.; Swern, D. *J. Org. Chem.* **1976**, *41*, 3329.

(5) Mancuso, A. J.; Brownfain, D. S.; Swern, D. *J. Org. Chem.* **1979**, *44*, 4148.

(6) In several related reactions it is worth noting that oxidation of lactone i with Me_2SO/TFAA[4] or with NCS/DMS[7] resulted in competing methylthiomethylation of the tertiary alcohol since mixtures of ii and iii were obtained. This problem could be circumvented by the use of pyridinium dichromate,[8] which gave only iv from v.

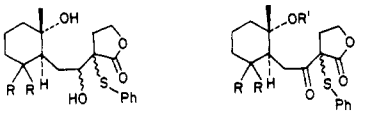

i R=H ii R=H, R'=H

v R=CH_3 iii R=H, R'=CH_2SCH_3

iv R=CH_3, R'=H

0022-3263/82/1947-4152$01.25/0